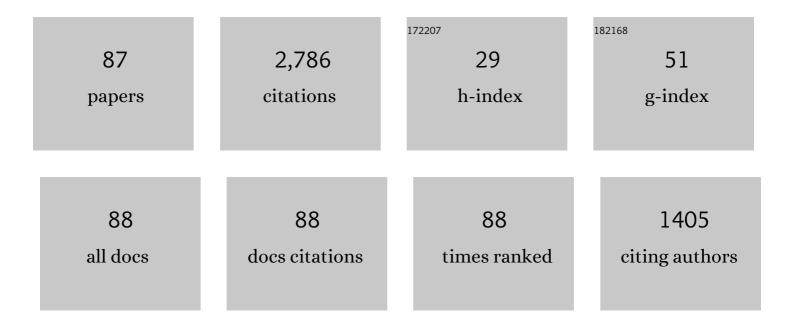
List of Publications by Year in descending order

Source: https://exaly.com/author-pdf/5834513/publications.pdf Version: 2024-02-01



#	Article	IF	CITATIONS
1	Immersed boundary method for the incompressible Reynolds Averaged Navier–Stokes equations. Computers and Fluids, 2022, 237, 105340.	1.3	4
2	10.1063/5.0088036.5., 2022,,.		0
3	10.1063/5.0088036.3. , 2022, , .		Ο
4	Vibrations of wind turbine blades in standstill: Mapping the influence of the inflow angles. Physics of Fluids, 2022, 34, .	1.6	15
5	10.1063/5.0088036.1., 2022,,.		ο
6	10.1063/5.0088036.2., 2022,,.		0
7	Stability analysis of vortex-induced vibrations on wind turbines. Journal of Physics: Conference Series, 2022, 2265, 042054.	0.3	3
8	A twoâ€dimensional quantitative parametric investigation of simplified surface imperfections on the aerodynamic characteristics of a NACA 63 ₃ â€418 airfoil. Wind Energy, 2021, 24, 310-322.	1.9	7
9	Fluid–structure interaction simulations of a wind turbine rotor in complex flows, validated through field experiments. Wind Energy, 2021, 24, 1426-1442.	1.9	15
10	Wind turbines in atmospheric flow: fluid–structure interaction simulations with hybrid turbulence modeling. Wind Energy Science, 2021, 6, 627-643.	1.2	11
11	Spectral analysis of New MEXICO standstill measurements to investigate vortex shedding in deep stall. Wind Energy, 2020, 23, 31-44.	1.9	1
12	Vortex induced vibrations of wind turbine blades: Influence of the tip geometry. Physics of Fluids, 2020, 32, .	1.6	33
13	Validation of blade-resolved computational fluid dynamics for a MW-scale turbine rotor in atmospheric flow. Journal of Physics: Conference Series, 2020, 1618, 052049.	0.3	7
14	Laminar-turbulent transition characteristics of a 3-D wind turbine rotor blade based on experiments and computations. Wind Energy Science, 2020, 5, 1487-1505.	1.2	8
15	Investigations of aerodynamic drag forces during structural blade testing using high-fidelity fluid–structure interaction. Wind Energy Science, 2020, 5, 543-560.	1.2	13
16	Laminarâ€ŧurbulent transition detection on airfoils by highâ€frequency microphone measurements. Wind Energy, 2019, 22, 1356-1370.	1.9	9
17	Suppressing Vortex Induced Vibrations of Wind Turbine Blades with Flaps. Springer Tracts in Mechanical Engineering, 2019, , 11-24.	0.1	9
18	Multipoint high-fidelity CFD-based aerodynamic shape optimization of a 10 MW wind turbine. Wind Energy Science, 2019, 4, 163-192.	1.2	49

#	Article	IF	CITATIONS
19	The influence of wing twist on pressure distribution and flow topology. Journal of Physics: Conference Series, 2018, 1037, 022036.	0.3	0
20	Aerodynamic effects of compressibility for wind turbines at high tip speeds. Journal of Physics: Conference Series, 2018, 1037, 022003.	0.3	6
21	Measured aerodynamic forces on a full scale 2MW turbine in comparison with EllipSys3D and HAWC2 simulations. Journal of Physics: Conference Series, 2018, 1037, 022011.	0.3	16
22	Investigation of droplet path in a rain erosion tester. Journal of Physics: Conference Series, 2018, 1037, 062030.	0.3	0
23	Inflow Turbulence and Leading Edge Roughness Effects on Laminar-Turbulent Transition on NACA 63-418 Airfoil. Journal of Physics: Conference Series, 2018, 1037, 022005.	0.3	5
24	A new kâ€epsilon model consistent with Monin–Obukhov similarity theory. Wind Energy, 2017, 20, 479-489.	1.9	27
25	Challenges in simulating coastal effects on an offshore wind farm. Journal of Physics: Conference Series, 2017, 854, 012046.	0.3	11
26	Why the Coriolis force turns a wind farm wake clockwise in the Northern Hemisphere. Wind Energy Science, 2017, 2, 285-294.	1.2	43
27	Why the Coriolis force turns a wind farm wake to the right in the Northern Hemisphere. Journal of Physics: Conference Series, 2016, 753, 032031.	0.3	2
28	Testing of selfâ€ s imilarity and helical symmetry in vortex generator flow simulations. Wind Energy, 2016, 19, 1043-1052.	1.9	37
29	Computing the flow past Vortex Generators: Comparison between RANS Simulations and Experiments. Journal of Physics: Conference Series, 2016, 753, 022014.	0.3	8
30	Simulations of wind turbine rotor with vortex generators. Journal of Physics: Conference Series, 2016, 753, 022057.	0.3	25
31	Experimental benchmark and code validation for airfoils equipped with passive vortex generators. Journal of Physics: Conference Series, 2016, 753, 022002.	0.3	23
32	CFD computations of the second round of MEXICO rotor measurements. Journal of Physics: Conference Series, 2016, 753, 022054.	0.3	29
33	Discontinuous Galerkin methodology for Large-Eddy Simulations of wind turbine airfoils. Journal of Physics: Conference Series, 2016, 753, 022037.	0.3	8
34	Modeling dynamic stall on wind turbine blades under rotationally augmented flow fields. Wind Energy, 2016, 19, 383-397.	1.9	23
35	Vortex-induced vibrations on a modern wind turbine blade. Wind Energy, 2016, 19, 2041-2051.	1.9	53
36	Fluid–structure interaction computations for geometrically resolved rotor simulations using CFD. Wind Energy, 2016, 19, 2205-2221.	1.9	53

#	Article	IF	CITATIONS
37	Aerodynamically shaped vortex generators. Wind Energy, 2016, 19, 563-567.	1.9	43
38	Comparison of OpenFOAM and EllipSys3D for neutral atmospheric flow over complex terrain. Wind Energy Science, 2016, 1, 55-70.	1.2	20
39	Predicting wind farm wake interaction with RANS: an investigation of the Coriolis force. Journal of Physics: Conference Series, 2015, 625, 012026.	0.3	15
40	An improved <i>k</i> ― <i>ϵ</i> model applied to a wind turbine wake in atmospheric turbulence. Wind Energy, 2015, 18, 889-907.	1.9	115
41	Comparison of wind turbine wake properties in nonâ€sheared inflow predicted by different computational fluid dynamics rotor models. Wind Energy, 2015, 18, 1239-1250.	1.9	62
42	Fully Consistent SIMPLE-Like Algorithms on Collocated Grids. Numerical Heat Transfer, Part B: Fundamentals, 2015, 67, 101-123.	0.6	9
43	The <i>k</i> - <i>ϵ</i> - <i>f</i> _{<i>P</i>} model applied to wind farms. Wind Energy, 2015, 18, 2065-2084.	1.9	42
44	The k - <i>ε</i> - f _{P} model applied to double wind turbine wakes using different actuator disk force methods. Wind Energy, 2015, 18, 2223-2240.	1.9	52
45	A study on rotational augmentation using CFD analysis of flow in the inboard region of the MEXICO rotor blades. Wind Energy, 2015, 18, 745-756.	1.9	27
46	Comments on the research article by Gross <i>et al.</i> (2012). Wind Energy, 2014, 17, 1985-1987.	1.9	0
47	Prediction of the Effect of Vortex Generators on Airfoil Performance. Journal of Physics: Conference Series, 2014, 524, 012019.	0.3	31
48	Fully consistent CFD methods for incompressible flow computations. Journal of Physics: Conference Series, 2014, 524, 012128.	0.3	3
49	Near wake Reynoldsâ€averaged Navier–Stokes predictions of the wake behind the MEXICO rotor in axial and yawed flow conditions. Wind Energy, 2014, 17, 75-86.	1.9	37
50	A simple atmospheric boundary layer model applied to large eddy simulations of wind turbine wakes. Wind Energy, 2014, 17, 657-669.	1.9	115
51	Verification and validation of an actuator disc model. Wind Energy, 2014, 17, 919-937.	1.9	67
52	An evaluation of several methods of determining the local angle of attack on wind turbine blades. Journal of Physics: Conference Series, 2014, 555, 012045.	0.3	24
53	Self-Similarity and helical symmetry in vortex generator flow simulations. Journal of Physics: Conference Series, 2014, 555, 012036.	0.3	2
54	A CFD code comparison of wind turbine wakes. Journal of Physics: Conference Series, 2014, 524, 012140.	0.3	3

#	Article	IF	CITATIONS
55	Design of the LRP airfoil series using 2D CFD. Journal of Physics: Conference Series, 2014, 524, 012020.	0.3	11
56	Canopy structure effects on the wind at a complex forested site. Journal of Physics: Conference Series, 2014, 524, 012112.	0.3	4
57	Transitional DDES computations of the NREL Phase-VI rotor in axial flow conditions. Journal of Physics: Conference Series, 2014, 555, 012096.	0.3	18
58	Comparison of wind turbine wake properties in non-uniform inflow predicted by different rotor models. Journal of Physics: Conference Series, 2014, 555, 012100.	0.3	2
59	Computation of the National Renewable Energy Laboratory Phaseâ€VI rotor in pitch motion during standstill. Wind Energy, 2012, 15, 425-442.	1.9	24
60	Characterization of the unsteady flow in the nacelle region of a modern wind turbine. Wind Energy, 2011, 14, 271-283.	1.9	46
61	The Bolund Experiment, Part II: Blind Comparison of Microscale Flow Models. Boundary-Layer Meteorology, 2011, 141, 245-271.	1.2	139
62	3D CFD computations of transitional flows using DES and a correlation based transition model. Wind Energy, 2011, 14, 77-90.	1.9	44
63	Hybrid RANS/LES applied to complex terrain. Wind Energy, 2011, 14, 225-237.	1.9	21
64	Investigation of the load reduction potential of two trailing edge flap controls using CFD. Wind Energy, 2011, 14, 449-462.	1.9	22
65	Imposing resolved turbulence in CFD simulations. Wind Energy, 2011, 14, 661-676.	1.9	12
66	CFD simulations of the MEXICO rotor. Wind Energy, 2011, 14, 677-689.	1.9	87
67	A stochastic model for the simulation of wind turbine blades in static stall. Wind Energy, 2010, 13, 323-338.	1.9	13
68	Hybrid RANS/LES method for wind flow over complex terrain. Wind Energy, 2010, 13, 36-50.	1.9	71
69	Design of a wind turbine rotor for maximum aerodynamic efficiency. Wind Energy, 2009, 12, 261-273.	1.9	54
70	CFD modelling of laminarâ€ŧurbulent transition for airfoils and rotors using the γ â^' model. Wind Energy, 2009, 12, 715-733.	1.9	109
71	Wind turbine rotorâ€ŧower interaction using an incompressible overset grid method. Wind Energy, 2009, 12, 594-619.	1.9	142
72	A CFD model of the wake of an offshore wind farm: using a prescribed wake inflow. Journal of Physics: Conference Series, 2007, 75, 012047.	0.3	9

#	Article	IF	CITATIONS
73	Aerodynamics and Characteristics of a Spinner Anemometer. Journal of Physics: Conference Series, 2007, 75, 012018.	0.3	5
74	On the Influence of Far-Wake Resolution on Wind Turbine Flow Simulations. Journal of Physics: Conference Series, 2007, 75, 012042.	0.3	20
75	Identification of severe wind conditions using a Reynolds Averaged Navier-Stokes solver. Journal of Physics: Conference Series, 2007, 75, 012053.	0.3	18
76	Hybrid RANS/LES Method for High Reynolds Numbers, Applied to Atmospheric Flow over Complex Terrain. Journal of Physics: Conference Series, 2007, 75, 012054.	0.3	8
77	Aerodynamic structures and processes in rotationally augmented flow fields. Wind Energy, 2007, 10, 159-178.	1.9	56
78	Hybrid RANS/LES of Neutral Atmospheric Boundary Layer: Simple Terrain. , 2007, , 155-158.		0
79	Enhancing the damping of wind turbine rotor blades, the DAMPBLADE project. Wind Energy, 2006, 9, 163-177.	1.9	17
80	New Insight Into the Flow Around a Wind Turbine Airfoil Section1. Journal of Solar Energy Engineering, Transactions of the ASME, 2005, 127, 214-222.	1.1	23
81	Aerofoil characteristics from 3D CFD rotor computations. Wind Energy, 2004, 7, 283-294.	1.9	130
82	Drag Prediction for Blades at High Angle of Attack Using CFD. Journal of Solar Energy Engineering, Transactions of the ASME, 2004, 126, 1011-1016.	1.1	32
83	AN IMPROVED SIMPLEC METHOD ON COLLOCATED GRIDS FOR STEADY AND UNSTEADY FLOW COMPUTATIONS. Numerical Heat Transfer, Part B: Fundamentals, 2003, 43, 221-239.	0.6	48
84	Detached-eddy simulation of flow around the NREL Phase VI blade. Wind Energy, 2002, 5, 185-197.	1.9	84
85	Navier-Stokes predictions of the NREL phase VI rotor in the NASA Ames 80 ft × 120 ft wind tunnel. Wind Energy, 2002, 5, 151-169.	1.9	289
86	Dynamic Stall on Rotating Airfoils: A Look at the N-Sequence Data from the NREL Phase VI Experiment. Key Engineering Materials, 0, 569-570, 611-619.	0.4	2
87	Validation of Aeroelastic Actuator Line for Wind Turbine Modelling in Complex Flows. Frontiers in Energy Research, 0, 10, .	1.2	5